Soft Matter

Accepted Manuscript

ROYAL SOCIETY OF CHEMISTRY

www.rsc.org/softmatter

ARTICLE TYPE www. rsc.org/xxxxxx | XXXXXXXX

Chain flexibility for tuning effective interactions in blends of polymers and polymer–grafted nanoparticles

Babji Palli and Venkat Padmanabhan*

Received Xth XXXXXXXXXX 20XX, Accepted Xth XXXXXXXXX 20XX
First published on the web Xth XXXXXXXXXX 200X
DOI: 10.1039/b000000x

We present molecular dynamics simulations of polymer–grafted nanoparticles in a homopolymer matrix to demonstrate the effect of chain flexibility on the potential of mean force (PMF) between various species in the nanocomposite. For a relatively high grafting density of Σ_g = 0.76 chains/σ_p^2 (where σ_p is the polymer monomer diameter), when the brush chain length is significantly smaller than ($<\sim 1/4$) the matrix chain length, the brushes exhibit autophobic dewetting with matrix polymers resulting in a strong attractive well in the particle–particle PMF. As the chain flexibility is decreased, we observe significant changes in particle–particle, particle–matrix, and brush–matrix PMFs that are strongly coupled with the length (or molecular weight) of grafted chains. For low molecular weight grafted chains, the change in the well–depth of particle-particle PMF, with increasing chain stiffness, is non–monotonous, while that for longer grafted chains (still shorter than matrix chains), the attractive well exhibits a monotonous decrease in its depth. The brush–matrix PMF and the matrix penetration depth into the brush layer indicate that wetting of grafted layer by matrix chains is enhanced with increasing chain stiffness.

1 Introduction

Tuning the macroscopic properties of polymer nanocomposites is highly desirable for applications in various sectors including electronics, photonics, battery, etc[1–4]. This is only possible when we establish a robust technique to dictate the microscopic morphology of nanoscale fillers within the polymer matrix. Different applications require different arrangement of nanoparticles that modifies certain property of the nanocomposite[5–7]. For example, mechanical stability is achieved by good dispersion of fillers in the matrix[4,8,9] whereas for applications in organic photovoltaics as active layer, a precise morphology is required to facilitate efficient exciton dissociation[10,11]. So, in order to design and engineer materials with highly desirable properties, it is crucial to have a strong control over the morphology of nanofillers within the polymer nanocomposite. To gain such control over the microscopic morphology, it is important to thoroughly understand the interparticle and polymer–particle interfacial interactions in greater detail. Computational tools have always been the preferred choice over experimental studies for understanding the fundamental phenomena, at a molecular level, responsible for such unique behavior of nanocomposites. This is primarily because it is extremely difficult to characterize and visualize constituents with that much detail in experiments. Many theoretical and simulation studies exist[8,12–20] that explore the effects of a vast set of molecular–level parameters including size and shape of fillers, grafting density, relative molecular weights of grafted and matrix chains, and graft–matrix heterogeneity, etc, on spatial organization and assembly/dispersion of polymer–grafted nanoparticles in a medium.

It is now well accepted, both theoretically[13,17,21–24] and experimentally[8,19,25,26], that functionalizing or grafting the nanoparticle surface with polymers that are compatible with the host matrix can significantly manipulate these interactions and thus control their spatial arrangement. Due to similarity in the chemical structures of graft and matrix polymers, one might expect to see a significant improvement in the effective miscibility of grafted particles in the matrix over that seen with 'bare' nanoparticles. However, there are several other parameters that dictate the final morphology of nanoparticles in a polymer matrix. In particular, at high grafting densities, grafted particles aggregate into spherical clusters if the brush molecular weight is much lower than the matrix molecular weight. At low grafting densities, the effective interparticle interaction is governed by the part of nanoparticle surface that is exposed and the part that is covered with grafted chains. Such homopolymer–grafted nanoparticles have shown to assemble into a variety of anisotropic nanostructures in solvent and in matrix[20]. Homogeneous dispersion of polymer–grafted nanoparticles in polymer matrix is achieved when the graft length is greater than approximately $1/4^{th}$ the length of matrix chains[27]. A more recent study[17] has shown that the polydispersity index (PDI) of grafted chains also has a strong effect on the effective interactions between polymer–grafted nanoparticles in a polymer matrix. The potential of mean force between grafted particles exhibits a reduction in the strength of both repulsion at contact and attraction at intermediate interparti-

cle distances, completely eliminating the latter at high PDI. The reduction in the mid–range attraction is attributable to the increased wetting of the grafted layer by matrix chains thus stabilizing the dispersion of grafted nanoparticles in the matrix.

Table 1 Mean end-to-end distance and persistence length of matrix polymers for various K values considered

K	$\langle R_e^2 \rangle^{1/2}$	L_p
0	7.95 ± 0.24	0.86 ± 0.05
1	9.07 ± 0.76	1.13 ± 0.12
2	10.92 ± 1.1	1.66 ± 0.03
3	13.08 ± 1.69	2.43 ± 0.28
4	15.27 ± 1.53	3.41 ± 0.26

Extensive amount of work exists on developing strategies for gaining control over the morphology of nanoparticles in a polymer matrix[11,19,21,26,28]. Most of computational studies have focused on blends with polymers modeled as freely–jointed flexible chains. However, several experimental polymers have different degrees of flexibility associated with their backbone. This leads to the question: Is chain flexibility an unimportant parameter to consider while trying to understand the fundamental behavior of nanocomposites? If no, does it have an effect large enough to alter the interparticle and polymer–particle effective interactions? In this article, we answer these questions by analyzing the particle–particle, particle–matrix, and brush–matrix potential of mean force (PMF) in polymer/grafted–particle blends with varying chain stiffness. Here, we only consider chains with low to moderate stiffness to avoid physical aggregation of chains dominated by their packing entropy. Our key finding is that for a relatively high grafting density, the autophobic dewetting of grafted particles and matrix polymers is significantly reduced by increasing the backbone rigidity of polymer chains.

2 Model and Methods

We used molecular dynamics (MD) simulations to study the effect of chain flexibility on the potential of mean force between various constituents in blends of polymer–grafted nanoparticles and homopolymer matrix. All simulations were carried out using the LAMMPS parallel MD package[29] in a cubic box with periodic boundary conditions in all directions. Both brush and matrix polymer chains were modeled as coarse–grained bead–spring chains, using the finite extensible nonlinear elastic (FENE) potential with standard values[30]. All monomers are chemically identical and have a mass m and diameter σ_p. Nanoparticles (NP) were represented as uniform spheres of diameter $\sigma_n = 4\sigma_p$. Polymer–grafted nanoparticles were then constructed by grafting N_g chains, with monomer diameter $\sigma_g = \sigma_p$, to the surface of each nanoparticle such that the grafting density, $\Sigma_g = 0.76$ chains/σ_p^2. The tethering beads were randomly distributed on the surface of nanoparticles. This was achieved by first applying a soft potential between nanoparticles and the tethering beads that push them slowly until the distance between their centers is equal to sum of the two radii[31]. From this point onwards, the tethering beads were fixed on the NP surface such that the nanoparticle core and the tethering beads act as one single entity. The degree of polymerization for matrix chains was kept constant at $M_m = 40$ and for grafted chains, we considered $M_g = 5$, 10, and 15. The number of matrix chains N_m and nanoparticles N_n were chosen such that the total packing fraction $\eta_T = \frac{\pi}{6}\left(\rho_p\sigma_p^3 + \rho_n\sigma_n^3 + \rho_g\sigma_g^3\right)$ and NP volume fraction $\phi_n = \rho_n\sigma_n^3 / \left(\rho_p\sigma_p^3 + \rho_n\sigma_n^3 + \rho_g\sigma_g^3\right)$ were kept constant at 0.415 (which corresponds to a melt–like condition) and 0.10, respectively. Chemically non–bonded pair–wise interactions between all particles in the system were defined using a shifted Lennard–Jones (LJ) potential. Athermal interaction was maintained between all particles in the system. The flexibility of chains was implemented through the semi–flexible chain model[32], with a bending potential given by $E_{bend} = K\left[1 + cos\theta\right]$ where, K is the bending energy and θ is the angle between two consecutive bonds. In this work, the flexibility of all chains was varied simultaneously to ensure that matrix and grafted polymers were of same type. The persistence length of chains corresponding to different K values considered in this study was calculated using

$$\langle R_e^2 \rangle = 2L_pL_c\left\{1 - \frac{L_p}{L_c}\left[1 - e^{-\left(L_c/L_p\right)}\right]\right\} \qquad (1)$$

where L_p is the persistence length, L_c is the contour length, and $\langle R_e^2 \rangle$ is the mean–squared end–to–end distance of the chains. The persistence length and the mean end–to–end distance of matrix chains are given in Table 1. All thermody-

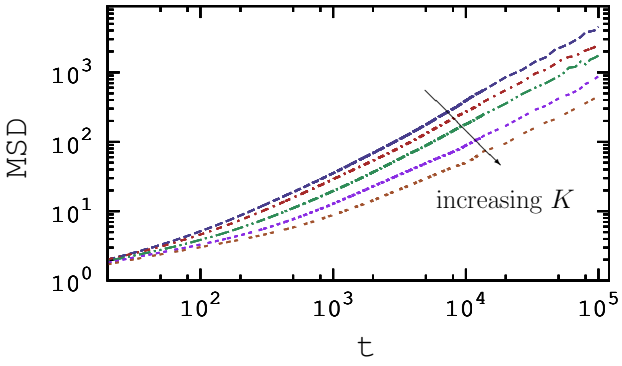

Fig. 1 Mean–squared displacement of nanoparticle core as a function of time during the equilibration step for $M_g = 15$. MSD for $M_g = 5$ and 10 were higher than those shown here.

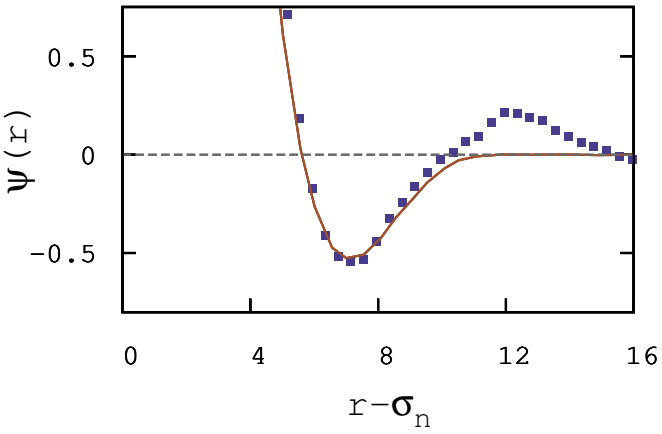

Fig. 2 Potential of mean force (in units of k_BT) between polymer grafted nanoparticles with M_g = 15 in a homopolymer matrix. The symbols represent PMF calculated from the pair correlation function and the line represents PMF calculated using the method described in Ref.[24].

namic quantities are expressed in reduced units that are convenient in molecular simulations. Each system was equilibrated for 5×10^7 MD steps with a $\delta t = 0.002$ such that the nanoparticles moved sufficiently across the simulation box as shown by their mean–squared displacement in Fig. 1.

3 Results and Discussion

We calculated the PMF between various constituents in blends of polymer–grafted nanoparticles and homopolymer matrix as $\Psi(r) = -k_BT\,[ln(g_{ij}(r))]$, where $g_{ij}(r)$ is the partial pair correlation function between species i and j and k_B is the Boltzmann constant. We note that this will only give an approximation of the actual PMF. As this method depends critically on the accuracy of the measured $g(r)$, we compared our results to the actual PMF between two polymer–grafted nanoparticles in a homopolymer matrix calculated following the work of Meng *et al.*[24]. Fig. 2 shows the PMF between nanoparticles with M_g = 15 calculated using the two methods. Although the well–depth obtained from both methods are in excellent agreement with each other, the PMF between the two nanoparticles calculated using the method described in Ref.[24] is 0 beyond a point when the grafted chains of the two nanoparticles are in contact. Whereas, in the case of PMF calculated using the pair correlation function, the non–zero values at high r are merely a manifestation of many body correlations in $g(r)$ due to the finite volume fraction of the nanoparticles. Thus, we emphasize here that the non–zero values in the PMF at high r are not meaningful.

The PMFs between polymer–grafted nanoparticles in blends with M_g = 5, 10, and 15 with varying chain flexibili-

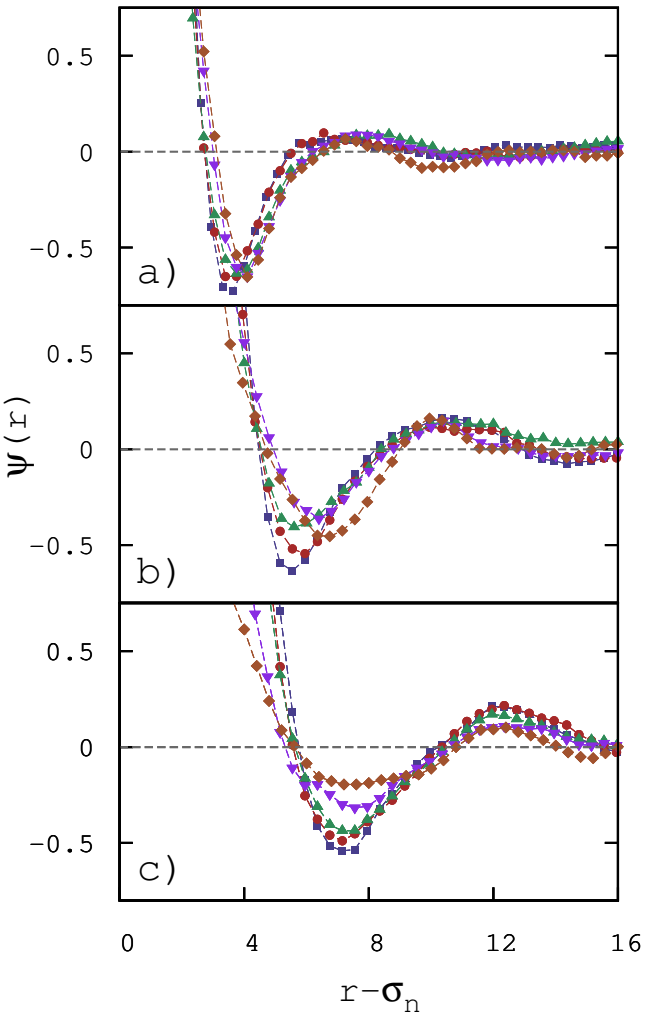

Fig. 3 PMF (in units of k_BT) as a function of interparticle distance $r - \sigma_n$ (in units of monomer diameter σ_p) between polymer–grafted nanoparticles ($\sigma_n = 4\sigma_p$) with Σ_g = 0.76 chains/σ_p^2, M_g = 5 (a), 10 (b), and 15 (c) for K = 0 (squares), 1 (circles), 2 (upward triangles), 3 (downward triangles), and 4 (diamonds) in a polymer/nanoparticle blend (η_T = 0.415) with M_m = 40.

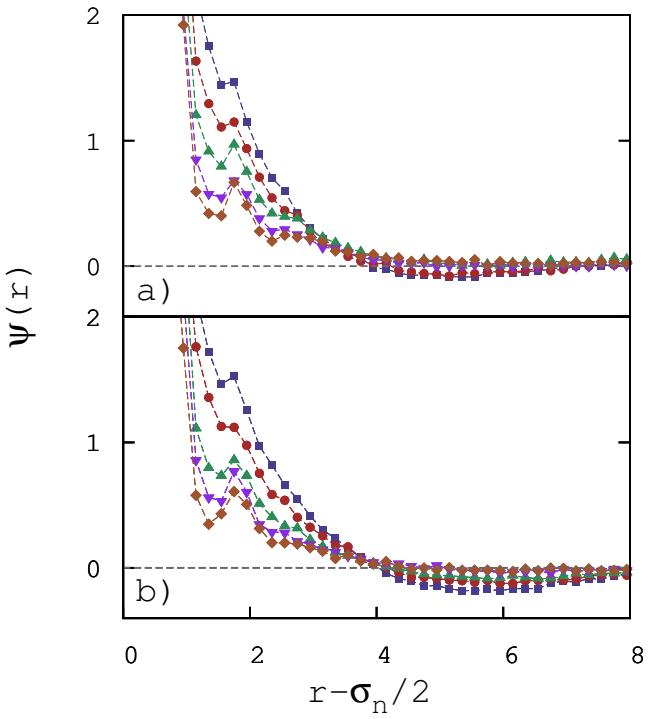

Fig. 4 PMF (in units of k_BT) as a function of interparticle distance $r - \sigma_n/2$ between nanoparticle–core and matrix polymers with M_g = 10 (a) and 15 (b) for K = 0 (squares), 1 (circles), 2 (upward triangles), 3 (downward triangles), and 4 (diamonds). The results for M_g = 5 are qualitatively similar.

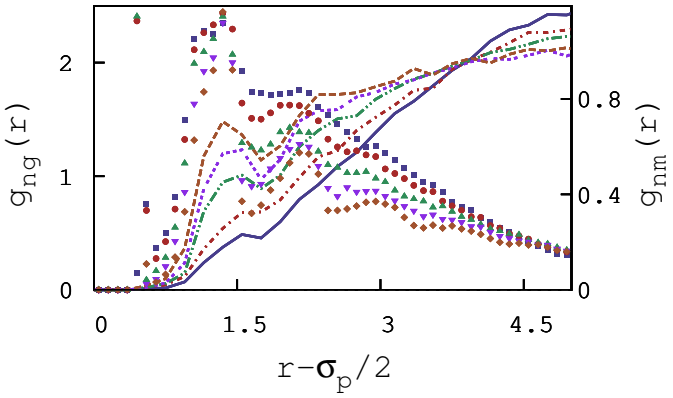

Fig. 5 Partial pair correlation functions between nanoparticle–grafts (left axis; symbols) and nanoparticle–matrix (right axis; lines) with M_g = 15 for K = 0 (squares, solid), 1 (circles, dash–dot), 2 (upward triangles, dash–dot–dot), 3 (downward triangles, dotted), and 4 (diamonds, dashed).

ties are shown in Fig. 3. It is now well–known that when the length (or molecular weight) of grafted chains is lower than that of matrix chains, the matrix dewets the grafted layer due to entropic factors, known as '*autophobic dewetting*'[24]. In this work, since all the grafted polymers were shorter than matrix polymers, we observe a similar dewetting phenomenon that is readily quantified by the presence of mid–range attractive well in the particle–particle PMF. The location of the attractive well at intermediate distances and not at contact is in accordance with the explanation provided by Kim *et al.*[33]. For all three lengths of grafted chains considered in this study, we also note that for freely jointed chains ($K = 0$; squares in Fig. 3), our results show that with increasing graft length, the attractive well in the PMF shifts to higher interparticle distances and the strength of attraction decreases. For systems with grafted chain lengths of M_g = 5 (Fig. 3a) and 10 (Fig. 3b), we observe that the strength of mid–range attraction between polymer–grafted nanoparticles exhibits a non–monotonous behavior with increasing stiffness. As we increase the stiffness, the depth of attractive well in the PMF decreases and beyond a certain value of K, it starts to increase again. This behavior is more prominent in case of M_g = 5, where the switch in the direction of change is observed for stiffness beyond $K = 2k_BT$. This non–monotonous behavior is probably because, for these systems with higher values of K, the persistence length becomes comparable to the length of grafted polymers and at these conditions, the system tries to compensate for the loss in chain configurational entropy due to stiffness. For systems with M_g = 15 (Fig. 3c), the length of grafted chains are significantly larger than their persistence length in which case, the configurational entropy is still the dominant contributor to the total free energy of the system and hence the change in PMF well–depth is monotonous in nature.

To understand why the mid–range attractive well–depth in the particle–particle PMF decreases with chain stiffness, we calculated the particle–matrix PMF as shown in Fig. 4. In all cases (including M_g = 5, which is not shown here to save space), we note that the repulsion at contact in the PMF decreases with chain flexibility. This significant drop and development of a well with increasing stiffness in the PMF indicates that the probability of locating a matrix monomer near the nanoparticle surface increases with chain stiffness. The development of a well in the PMF at $r - \sigma_n/2$ = 1 indicates that there is some layering of matrix monomers on top of tethered beads of grafted chains and the drop in the repulsion at contact can be attributed to enhanced wetting of grafted layer by matrix polymers. To confirm this, we calculated the partial pair correlation functions between nanoparticle–graft and nanoparticle matrix for all three cases. The pair correlation functions for M_g = 15 are shown in Fig. 5 (pair correlation functions for M_g = 5 and 10 are qualitatively similar and are hence not shown here). It is evident from this figure that as we increase the chain stiffness, the density of matrix chains near the nanoparticle core increases and for higher values of K (3

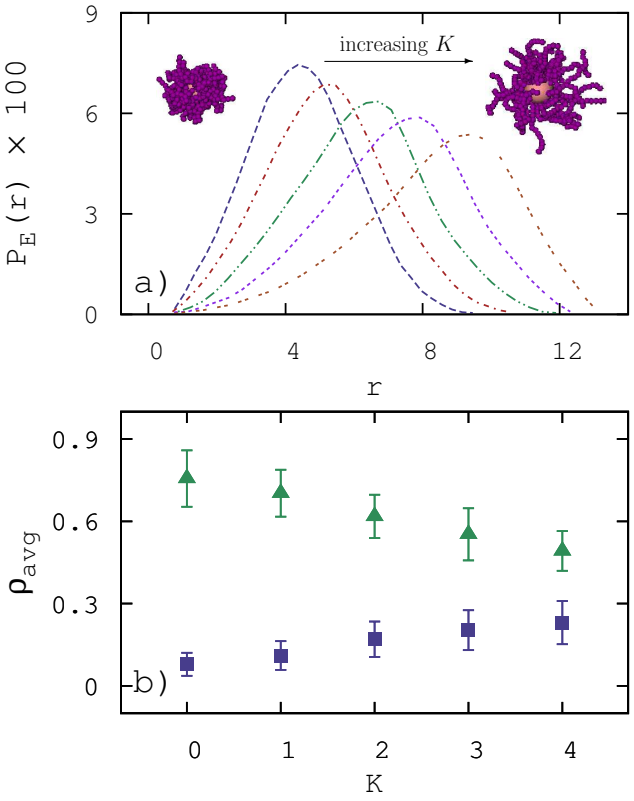

Fig. 6 a) Probability distribution of end–monomers of grafted chains with $M_g = 15$ as a function of distance r from the surface of nanoparticles. The grafted chains are folded for $K = 0$, to minimize interaction with matrix monomers, while for $K = 4$, the chains are forced to stretch which in turn facilitates penetration of matrix chains into the grafted layer. b) Average density of graft (triangles) and matrix (squares) monomers surrounding nanoparticles within a region of thickness equal to corresponding graft height.

and $4k_BT$ for $M_g = 15$), the local density is higher than the matrix bulk density.

In all systems considered here, as $M_g < M_m$, when $K = 0$, we find that the grafted chains tend to minimize their interaction with matrix chains by folding as much as possible to avoid contact with the matrix monomers that is evident from the end–monomer probability distribution, shown in Fig. 6a, of grafted chains as a function of distance from the surface of nanoparticle. Now, as we increase the chain stiffness, we note that there is a significant shift in the end–monomer probability distribution as a result of stretching of grafted chains. The entropic contribution to the dewetting mechanism is significantly lowered as the associated stiffness of backbone causes the chains to stretch farther and facilitate penetration of matrix chains into the grafted layer. The region surrounding a nanoparticle, which was predominantly occupied by grafted monomers in the $K = 0$ case, is now being shared by both

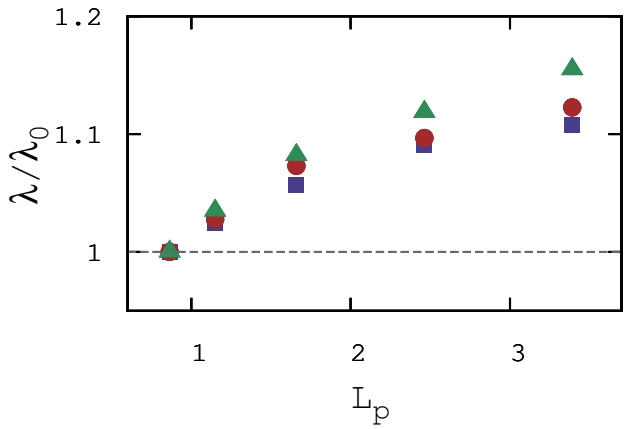

Fig. 7 Penetration depth of matrix polymers into the grafted layer on nanoparticles as a function of chain persistence length for systems with $M_g = 5$ (squares), 10 (circles), and 15 (triangles). λ_0 is the penetration depth of freely–jointed chains ($K = 0$).

grafted and matrix monomers for $K = 4k_BT$ resulting in the wetting phenomenon. This can be clearly seen in Fig. 6b that shows the average density of grafted and matrix monomers in the region surrounding a nanoparticle from its surface to a distance equal to the corresponding brush height h_g. As the stiffness of chains is increased, the density of graft monomers surrounding the nanoparticle decreases, while the density of matrix monomers increases. Next, we quantify the enhancement of wetting by estimating the average distance the matrix chains penetrate into the grafted layer by calculating the matrix penetration depth as

$$\lambda = \sqrt{\frac{\int_0^{h_g} r^2 g_{nm}(r) dr}{\int_0^{h_g} g_{nm}(r) dr}} \qquad (2)$$

where, $g_{nm}(r)$ is the nanoparticle–matrix partial pair correlation function and h_g is the brush height. The penetration depth λ, as shown in Fig. 7, increases for all three cases with increasing chain stiffness.

4 Summary and Conclusions

In summary, this is one of the first studies that demonstrates the effect of chain flexibility on the PMF between various constituents in blends of polymer–grafted nanoparticles and homopolymer matrix. For various lengths of grafted chains considered in this study, our results show that chain flexibility has a profound impact on the wettability of grafted chains by matrix polymers. For low molecular weight grafts (short chains), although the penetration of matrix polymers into the grafted layer is enhanced with increasing stiffness, the particle–particle PMF shows a non-monotonous behavior

as the persistence length becomes comparable to the grafted chain length. When the length of grafted chains is significantly larger than their persistence length, the increase in matrix penetration depth with chain stiffness is directly responsible for decrease in the well–depth of particle–particle PMF leading to enhanced wetting and dispersion of polymer–grafted nanoparticles in homopolymer matrix. For slightly lower grafting densities, reduced chain flexibility might significantly decrease the well–depth in particle–particle PMF as the brushes undergo a greater amount of stretching in these cases. This work motivates the selection of right set of parameters including relative molecular weights of polymers depending on the backbone stiffness of polymer in hand that could potentially stabilize nanoparticles where aggregation is usually observed.

Acknowledgements

This work was partially supported by the Department of Chemical Engineering at the Indian Institute of Technology Kharagpur. The authors also acknowledge the High Performance Computing Center (HPCC) at Texas Tech University at Lubbock for providing HPC resources that have contributed to the research results reported within this paper. URL: http://www.hpcc.ttu.edu.

References

1 M. A. C. Stuart, W. T. S. Huck, J. Genzer, M. Muller, C. Ober, M. Stamm, G. B. Sukhorukov, I. Szleifer, V. V. Tsukruk, M. Urban, F. Winnik, S. Zauscher, I. Luzinov and S. Minko, *Nat. Mater.*, **9**, year.
2 S. Liu and Z. Tang, *J. Mater. Chem.*, 2010, **20**, 24–35.
3 A. C. Power, A. J. Betts and J. F. Cassidy, *Analyst*, **135**, year.
4 A. J. Crosby and J. Y. Lee, *Polym. Rev.*, 2007, **47**, 217–229.
5 J. Jancar, J. F. Douglas, F. W. Starr, S. K. Kumar, P. Cassagnau, A. J. Lesser, S. S. Sternstein and M. J. Buehler, *Polymer*, 2010, **51**, 3321–3343.
6 R. A. Vaia and J. F. Maguire, *Chem. Mater.*, 2007, **19**, 2736–2751.
7 M. Seul and D. Andelman, *Science*, 1995, **267**, 476–483.
8 M. E. Mackay, A. Tuteja, P. M. Duxbury, C. J. Hawker, B. V. Horn, Z. Guan, G. Chen and R. S. Krishnan, *Science*, 2006, **311**, 1740–1743.
9 P. H. T. Vollenberg and D. Heikens, *Polymer*, 1989, **30**, 1656–1662.
10 T. T. T. N. N. Dinh, D. N. Chung and D. Hui, *J. Nanomaterials*, 2012, **2012**, 190290.
11 X. C. Chen and P. F. Green, *Langmuir*, 2010, **26**, 3659–3665.
12 K. Yoshimoto, T. S. Jain, K. V. Workum, P. F. Nealey and J. J. de Pablo, *Phys. Rev. Lett.*, 2004, **93**, 175501.
13 S. E. Harton and S. K. Kumar, *J. Polym. Sci., Part B: Polym. Phys.*, 2008, **46**, 351–358.
14 Z. Y. Tang, Z. L. Zhang, Y. Wang, S. C. Glotzer and N. A. Kotov, *Science*.
15 J. Y. Lee, A. C. Balazs, R. B. Thompson and R. M. Hill, *Macromolecules*, 2004, **37**, 3536–3539.
16 S. C. Glotzer and M. J. Solomon, *Nature Mater.*, 2007, **6**, 557–562.
17 T. B. Martin, P. M. Dodd and A. Jayaraman, *Phys. Rev. Lett.*, 2013, **110**, 018301.
18 A. Bansal, H. Yang, C. Li, B. C. Benicewicz, S. K. Kumar and L. S. Schadler, *J. Polym. Sci. B*, 2006, **44**, 2944–2950.
19 C. K. Wu, K. L. Hultman, S. O'Brien and J. T. Koberstein, *J. Am. Chem. Soc.*, 2008, **130**, 3516–3520.
20 P. Akcora, H. Liu, S. K. Kumar, J. Moll, Y. Li, B. C. Benicewicz, L. S. Schadler, D. Acehan, A. Z. Panagiotopoulos, V. Pryamitsyn, V. Ganesan, J. Ilavsky, P. Thiyagarajan, R. H. Colby and J. F. Douglas, *Nat. Mater.*, 2009, **8**, 354–359.
21 J. Kalb, D. Dukes, S. K. Kumar, R. S. Hoy and G. S. Grest, *Soft Matter*, 2011, **7**, 1418–1425.
22 J. J. Xu, F. Qiu, H. D. Zhang and Y. L. Yang, *J. Polym. Sci., Part B: Polym. Phys.*, 2006, **44**, 2811–2820.
23 D. M. Trombly and V. Ganesan, *J. Chem. Phys.*, 2010, **133**, 154904.
24 D. Meng, S. K. Kumar, J. M. D. Lane and G. S. Grest, *Soft Matter*, 2012, **8**, 5002–5010.
25 D. L. Green and J. Mewis, *Langmuir*, 200621, **22**, 9546–9553.
26 J. Kim and P. F. Green, *Macromolecules*, 2010, **43**, 1524–1529.
27 C. Chevigny, F. Dalmas, E. D. Cola, D. Gigmes, D. Bertin, F. Boue and J. Jestin, *Macromolecules*, 2011, **44**, 122–133.
28 L. M. Hall, A. Jayaraman and K. S. Schweizer, *Curr. Opin. Solid State Mater. Sci.*, 2010, **14**, 38–48.
29 S. Plimpton, *J. Comput. Phys.*, 1995, **117**, 1–19.
30 G. S. Grest and K. Kremer, *Phys. Rev. A*, 1986, **33**, 3628.
31 K. Kremer and G. S. Grest, *J. Chem. Phys.*, 1990, **92**, 5057–5086.
32 K. Honnell, J. G. Curro and K. S. Schweizer, *Macromolecules*, 1990, **23**, 3496–3505.
33 J. U. Kim and M. W. Matsen, *Macromolecules*, 2008, **41**, 4435–4443.